J Mater Sci (2010) 45:5950–5959
DOI 10.1007/s10853-010-4680-4

Insulation capability of the bark of trees with different fire adaptation

Georg Bauer · Thomas Speck · Jan Blömer · Jürgen Bertling · Olga Speck

Received: 26 March 2010 / Accepted: 28 May 2010 / Published online: 17 July 2010

Abstract When exposed to a surface fire, the probability of a tree to survive widely varies, depending on its capability to protect the cambium from lethal temperatures above 60 °C. Thereby, the bark, the entirety of all tissues outside the cambium, serves as an insulation layer. In laboratory experiments, the heat production of a surface fire was simulated and the time span τ_{60} until the temperature of 60 °C is reached in the inner bark surface was measured. Thereby, τ_{60}—as a measure of the fire resistance—was quantitatively determined for seven tree species. In addition, the influence of bark thickness and moisture content on bark heat insulation capacities was examined. Independent of the tree species and bark moisture content a power function correlation between bark thickness and τ_{60} was found. Our results also show that fire resistance increases with decreasing bark density. The seven tree species examined can be classified in two groups differing highly significant in their bark structure: (1) tree species with a faintly structured bark, which show a low fire resistance, and (2) tree species with an intensely structured bark, showing a high fire resistance. Furthermore a mathematical model simulating heat conduction was applied to describe the experimental results, and some ideas for a transfer into biomimetic materials are presented.

G. Bauer · T. Speck · O. Speck (✉)
Plant Biomechanics Group, Botanic Garden, Faculty of Biology, University of Freiburg, Schänzlestraße 1, 79104 Freiburg, Germany
e-mail: olga.speck@biologie.uni-freiburg.de

T. Speck · J. Bertling · O. Speck
Bionics Competence Network BIOKON e.V., Berlin, Germany

T. Speck · O. Speck
Competence Network Biomimetics, Freiburg, Germany

J. Blömer · J. Bertling
Fraunhofer Institute for Environmental, Safety, and Energy Technology UMSICHT, Osterfelder Straße 3, 46047 Oberhausen, Germany

Introduction

Forest fires are often looked upon as disasters despite their natural occurrence, millennia-long use by man and importance in many ecosystems [1, 2]. Especially low intensity surface fires with typical temperatures between 200 and 220 °C (in some cases considerably higher temperatures up to 400 °C can occur [3, 4]) may facilitate the breaking of cones, reduce parasites and fungal infections, kill competing sprouts, and contribute to higher substrate turnover rates. Fast moving surface fires result in low heat development, whereas ground fires burn the humus layer of the forest ground with temperatures of more than 500 °C and thus kill the entire living substance. Crown fires, another type of forest fire, may lead to lethal effects by transferring the heat to the ground, which results in critical ground temperatures. Thus, surface fires are the only type of forest fires which plants can survive to a substantial percentage [3].

For trees, most of the lethal situations during surface fires occur when the temperature of the cambium increases above 60 °C. Thus, as the ecologically important factor is to prevent the cambium from exceeding this temperature, the fire resistance of a tree can be characterized by the time span, τ_{60}, until the temperature in its cambium exceeds 60 °C [5]. The bark, a term here used to describe the entirety of the outer tissue layers of a tree, peripheral to the cambium, determines a trees fire resistance by its heat

insulation capacity. Dimitri [6] showed that for beeches insulation capacity depends, among other things, on the varying moisture content of the bark.

Several field experiments have been conducted regarding trees' adaptations to survive surface fires. Hare introduced in 1965 a method to examine bark heat insulation by burning a kerosene–motoroil-soaked rope that was wrapped around an instrumented tree while temperatures of cambium and bark surface were measured by thermocouples [7]. For further experimental set-ups, a modified wick-fire technique was used [e.g., 8, 9]. To avoid unacceptably high levels of heat output variations during these methods, Van Mantgem and Schwartz [5] used an electrical copper pad instead of a wick-fire for bark surface heating. A laboratory approach to examine fire resistance was suggested by Gill and Ashton [10], who applied radiant heat by electrically heated elements. The heat source was kept at a constant distance from the bark.

In several previous studies, it was determined that fire resistance is mainly correlated with bark thickness, and that interspecific differences in other physical bark properties affect its fire resistance only negligibly [e.g., 5, 11, 12]. A linear correlation between bark thickness and fire resistance was found by Harmon [13] and for two out of three tree species examined by Gill and Ashton [10]. Contradictory to these findings are the results of Van Mantgem and Schwarz [5] and Hare [7], indicating an exponential correlation, as well as those for the third tree species examined by Gill and Ashton [10], where a curvilinear relationship is mentioned.

In this study, heat insulation capacities of seven tree species were examined in the laboratory by simulating the fire intensity of a surface fire with a Bunsen burner. The influence of bark thickness and moisture content on heat insulation was studied and compared to the results derived from a one-dimensional mathematical model for dry bark simulating a forest fire. Comparative experiments showed the influence of relative humidity during storage on bark moisture content. Additional properties such as bark density and bark structure were determined for further characterization of the bark.

Materials and methods

Materials

The tree species used in this work were chosen because of the different fire regimes of their natural distribution area: *Quercus suber* L. (Cork Oak) and *Sequoiadendron giganteum* Lindl. (Giant Sequoia) are native in areas where forest fires are common with a fire period of a few years, whereas forest fires do not play a decisive role in the distribution areas of *Fagus sylvatica* L. (Common Beech), *Abies alba* Mill. (European Silver Fir), and *Tilia cordata* Mill. (Little Leaf Linden). *Pinus sylvestris* L. (Scots Pine) and *Larix decidua* Mill. (European Larch) are native in areas where forest fires may occur, but not to the extent as in the distribution areas of the first mentioned species. Bark of 1–2 freshly felled specimens per tree species, each 21–32-years-old, was peeled off at a height of about 40–120 cm above ground and stored in plastic bags to avoid desiccation. All the trees felled were chosen as being representative for their tree species with regard to their stem and bark structure. We limited the sample size to 1–2 specimens per tree species to avoid an excessive felling of trees. The bark was taken as far down as to the cambium. That means that the test specimens consisted of inner and outer bark, which may be traversed by layers of secondarily developed protective bark tissue called periderm. Samples of *Quercus suber* were bought, so in this case age, height above ground, and the exact tissue composition of the specimen could not be specified.

Bark moisture content

The fresh weight of 22 bark samples from *F. sylvatica*, *T. cordata*, *P. sylvestris*, and *L. decidua* (5 to 6 samples from each tree species) was measured, afterward the samples were dried by decreasing the relative humidity (rH) of the storage sites in six steps, from 100% rH to 0% rH (oven-dried). When stored under a constant rH, samples level out at a certain moisture content. Due to a hysteresis effect between adsorption and desorption, this moisture content differs between samples that were wetted and, as in our case, samples that were dried to reach this moisture content. After each step all samples were weighted and the bark moisture content F_0 of each sample was calculated from

$$F_0 = \frac{m_u - m_0}{m_0} \quad (1)$$

where m_u is the mass of the moist sample and m_0 is the mass of the dry sample, respectively. The averaged bark moisture content of each step was compared to that of fresh bark samples to find the storage condition under which bark samples show a moisture content similar to that of fresh samples. In order to assess the ecological conditions under which the fresh bark samples were collected, the precipitation of the 22 days preceding sampling was recorded.

Surface fire simulation—τ_{60} a measure of fire resistance

Additional bark samples were divided into two groups and stored under different conditions: about half of the samples

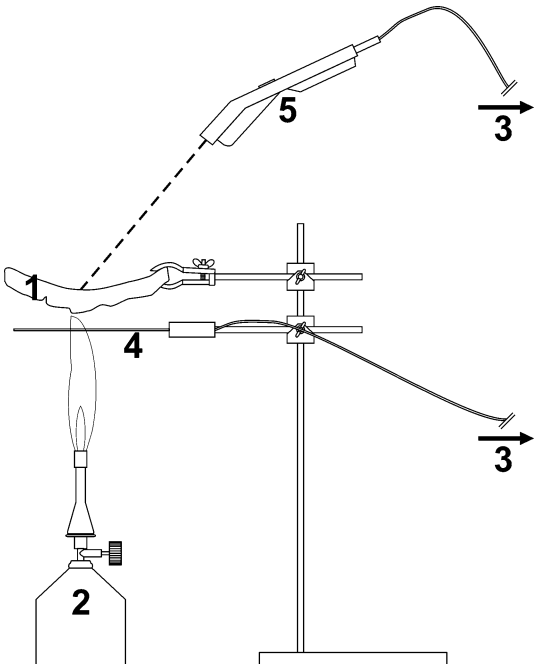

Fig. 1 Schematic drawing of the experimental set up for fire resistance analyses. A bark sample (*1*) was placed in a height of 43 cm over a Bunsen burner, the flame length was about 20 cm (*2*). A computer (*3*) recorded both the flame temperature, measured by a thermocouple (*4*), and the temperature of the inner bark surface, i.e., the position of the cambium in the living tree, measured contactless by an infrared thermometer (*5*)

were stored in a box with 100% rH, the rest were oven-dried prior to the surface fire simulations. The bark samples were placed over a Bunsen burner with their outer surface facing downward (Fig. 1). Temperatures of both the inner bark surface and the flame were measured by an infrared thermometer and a thermocouple, respectively, and recorded by a computer after the Bunsen burner was lit. Flame temperatures of 93 experiments were recorded, showing a mean value of 214.6 ± 20.2 °C which is in good accordance with temperatures measured for low intensity surface fires. The experiment ended as soon as the inner bark surface exceeded 60 °C or after 21 min if this temperature was not reached. Thereafter, bark thickness at the position heated was measured and the time span, τ_{60}, as a measure of the fire resistance was recorded. For each storage condition, the hypothesis of a linear and a power function correlation between τ_{60} and bark thickness were compared using a R^2 fit. The period of time of 21 min was chosen to cover a duration which is well beyond that of the heat peak in typical surface fires which are known to last between 2 and 9 min [8, 14].

Bark structure

For all samples the minimum and maximum bark thicknesses ($D_{\min}$ and $D_{\max}$) as well as two values of bark thickness at randomly chosen points were measured. From these four values, s as a measure of the surface structure of the bark was calculated for each bark sample from

$$s = \frac{D_{\max} - D_{\min}}{D_0} \tag{2}$$

where D_0 is the mean value of all four values mentioned above. The standard deviation of s was calculated from the standard deviations of $D_{\min}$, $D_{\max}$, and D_0. As higher s as more pronounced is the surface structuring of a given bark sample.

Bark density

Air-dried bark samples were used to calculate bark gross density, ρ, including bark cavities, from

$$\rho = \frac{m}{V} \tag{3}$$

where m is the weight and V the volume of each sample, measured by xylometric methods [15].

Modeling of dry bark

For dry bark a simple, one-dimensional, finite volume model is applied to describe the experimental results. Therefore, the bark is divided in slices (typically 50) and for each slice the energy balance is applied (Fig. 2).

$$\frac{\partial E}{\partial t} = A\left(\mathrm{Flux}_{\mathrm{left}} - \mathrm{Flux}_{\mathrm{right}}\right) \tag{4}$$

with the energy $E = \rho c_p T A \mathrm{d}x$, the cross section A, the density ρ, the heat capacity c_p, the temperature T and the length coordinate x.

The fluxes inside the bark are described by Fick's law of heat conduction

$$\mathrm{Flux} = -\lambda \frac{\partial T}{\partial x} \tag{5}$$

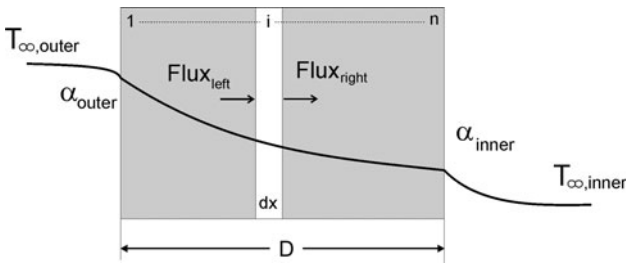

Fig. 2 Sketch of the model with bark thickness, D, for n bark slices dx with the constant temperatures of the outer side ($T_{\infty,outer}$) and inner side ($T_{\infty,inner}$) of the bark. The heat transfer coefficient at the outer side α_{outer} is assumed to be much higher than the coefficient at the inner side α_{inner} because of the direct contact to the flame

with the heat conductivity λ, and the fluxes at the outer and inner side of the bark are described by a constant heat transfer coefficient

$$\begin{aligned}\text{Flux}_{\text{outer}} &= \alpha_{\text{outer}}\left(T_{\infty,\text{outer}} - T_1\right) \text{Flux}_{\text{inner}} \\ &= \alpha_{\text{inner}}\left(T_n - T_{\infty,\text{inner}}\right)\end{aligned} \tag{6}$$

The heat transfer coefficient at the outer side, α_{outer}, is assumed to be very high because of the direct contact to the flame. In the model it is set to 100 times the coefficient at the inner side, α_{inner}. Furthermore, the length coordinate x is scaled by the thickness of the bark D.

$$\tilde{x} = \frac{x}{D} \tag{7}$$

All parameters (λ, ρ, c_p, ε) are assumed to be constant for one sample. The bark density, ρ, was measured by xylometric methods and the porosity is calculated by assuming a constant density of the solid matter within the bark of $\rho_0 = 1460\text{kg/m}^3$ [11]. The porosity calculates to

$$\varepsilon = 1 - \frac{\rho}{\rho_0} \tag{8}$$

The heat capacity of the solid matter $c_{p,0} = 1500\,\text{J/kgK}$, an average value for the interesting temperature range, is assumed to be same for all samples [16]. Introducing Eqs. 5–7 into Eq. 4 and rearranging yields

$$\begin{aligned}\frac{\partial T_1}{\partial t} &= \frac{\alpha_{\text{outer}}}{\rho c_p D}\left(T_{\infty,\text{outer}} - T_1\right) + \frac{\lambda}{\rho c_p D^2}\frac{\partial T_1}{\partial \tilde{x}} \\ \frac{\partial T_i}{\partial t} &= -\frac{\lambda}{\rho c_p D^2}\left(\frac{\partial T_i}{\partial \tilde{x}} - \frac{\partial T_{i+1}}{\partial \tilde{x}}\right), \quad i = 2,\ldots,n-1 \\ \frac{\partial T_n}{\partial t} &= -\frac{\lambda}{\rho c_p D^2}\frac{\partial T_{n-1}}{\partial \tilde{x}} - \frac{\alpha_{\text{inner}}}{\rho c_p D}\left(T_n - T_{\infty,\text{inner}}\right)\end{aligned} \tag{9}$$

Due to the assumed excellent heat transfer in the flame, the outer side of the bark reaches the final, constant temperature nearly immediately. In this case, the specific choice of α_{outer} does not influence the transient temperature profiles in the bark, and it is not considered for the interpretation of the results. Therefore, the profiles are determined by two remaining constants only

$$\begin{aligned}A &= \frac{\lambda}{\rho c_p D^2} \\ B &= \frac{\alpha_{\text{inner}}}{\rho c_p D}\end{aligned} \tag{10}$$

Equation 9 is solved by an ordinary 4th order Runge–Kutta-scheme [17].

The heat transfer coefficient at the inner side is assumed to be the same for all samples while the heat conductivity differs from specimen to specimen naturally. Therefore, the heat conductivity has to be related to properties of the bark. Here two models were considered: either the heat conductivity varies linearly with the porosity ε of the bark between the conductivity of air, λ_{air}, and the conductivity of the pure bark material, λ_0, or a more complicated model of Eucken is applied which was already used by Martin [11]:

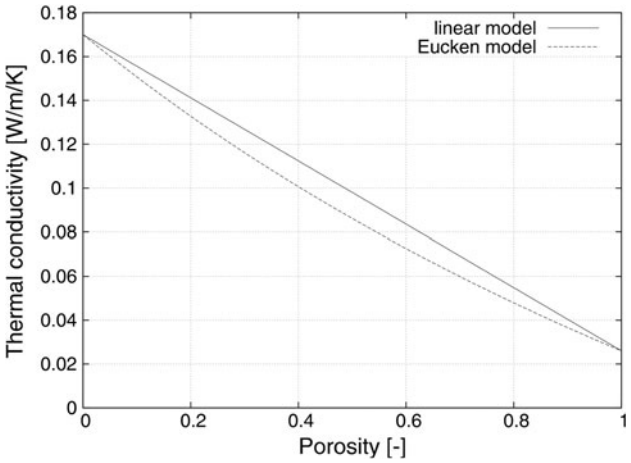

Fig. 3 Heat conductivity versus porosity. Both a linear model and Eucken's model are shown

$$\lambda = \lambda_0(1-\varepsilon) + \lambda_{\text{air}}\varepsilon \quad \lambda = \lambda_0\frac{1 - 2\varepsilon\left(\frac{\lambda_0-\lambda_{\text{air}}}{2\lambda_0+\lambda_{\text{air}}}\right)}{1 + \varepsilon\left(\frac{\lambda_0-\lambda_{\text{air}}}{2\lambda_0+\lambda_{\text{air}}}\right)}$$

In principal the porosity is not sufficient to calculate the heat conductivity exactly because the exact inner structure of the bark had to be considered but no data are available, yet. Therefore, the Eucken model is chosen (Fig. 3).

A genetic algorithm is applied [18] to fit λ_0 and α_{inner} to all results simultaneously. Therefore, a least square fit of the time τ_{60} to reach 60 °C at the inner side was applied. Due to the big range of τ_{60} normalized residuals are used.

$$\text{Residuum} = \sum_N \left(\frac{\tau_{60,\text{exp}} - \tau_{60,\text{mod}}}{\tau_{60,\text{exp}}}\right)^2 \Rightarrow \text{Min}$$

Statistics

The following statistical analyses were performed with SPSS (version 15.0.1. 2006, SPSS Inc., Chicago, Illinois, USA). Moisture content of fresh samples was compared to that of samples stored at 100% rH by a *t*-test. Interspecific differences in bark thickness, τ_{60}, bark structure as well as bark density were examined by Tamhane post hoc tests. As significance level $p = 0.05$ was chosen, subdivided into: $p < 0.05$ (less significant), $p < 0.01$ (significant) and $p < 0.001$ (highly significant). A best subsets regression was performed describing the influence of bark thickness, bark density, and bark structure on τ_{60} using SigmaStat Version 3.10.0 (Systat Software Inc.). All mean values are given with standard deviations.

Results

Bark moisture content

In order to determine the dependency of the moisture content of the bark from the relative humidity of the storage sites, the mean value of bark moisture content found at each step of drying is plotted against the rH of the storage sites (Fig. 4). The relation between rH and water content can be described in good approximation by a polynomial interpolation of degree 3 ($R^2 = 0.95$). Based on this relation, the moisture content of the bark could be adjusted in the laboratory by choosing the respective relative humidity for storage. To adjust the moisture content of bark used in the laboratory as close as possible to that of fresh bark (95.2 ± 24.6%), the bark samples were stored at a rH of 100%, where an average moisture content of 92.1 ± 23.8% is reached. The total precipitation of the 22 days preceding sampling added to 51.6 l/m^2 and thus assured a characteristic bark moisture content for this period of the year (early August).

Surface fire simulation—τ_{60} a measure of fire resistance

The inner surface (according to the position of the cambium in the living tree) of 64 out of 67 tested oven-dried bark samples stored at 0%rH (exception: three samples of *S. giganteum*) reached 60 °C within 21 min. The same holds also for 60 out of 72 wet bark samples stored at 100% rH (exception: one bark sample of *L. decidua* as well as all 11 bark samples of *S. giganteum* for which τ_{60} is not reached within the testing time of 21 min). For these samples, τ_{60} is measured and mean values of each species are plotted against bark thickness (Fig. 5). Sample sizes, mean values, and standard deviations are attached in Appendix. *S. giganteum* and *Q. suber*, which are most often exposed to wild fires in their natural habitat show the best fire resistance which is mirrored by the highest values found for τ_{60} (for wet bark samples of *S. giganteum* τ_{60} is not even reached within the testing period of 21 min). The τ_{60}-values of these two species do not differ significantly but are significantly higher for dry bark than the values found in all other tested species with the exception of *L. decidua* (Table 1). *P. sylvestris* and *L. decidua* distributed in regions where wild fires occur regularly but not very often show the third and fourth highest values of τ_{60} of the seven tested tree species. The three species from natural habitats where wild fires occur very rarely if at all show the three lowest values of τ_{60}. The lowest values as well for dry and moist bark are found in *F. sylvatica*, the second lowest values in *A. alba.* The τ_{60}-values for dry and moist bark are not significantly different between these two species but are significantly lower than in all other tested species (Table 1). The third lowest τ_{60}-value occurs in *T. cordata* which yet is significantly higher than the values found for the two other species from habitats with a low probability of wild fires. The τ_{60}-values of *T. cordata* are more similar to those found for *P. sylvestris* and *L. decidua*. The correlation of bark thickness, D, and τ_{60} can be described by a power function correlation with exponents close to 1 ($\tau_{60} = 36.0 \cdot D^{1.253}$ with $R^2 = 0.90$ for wet bark and $\tau_{60} = 9.1 \cdot D^{1.401}$ with $R^2 = 0.95$ for dry bark). In

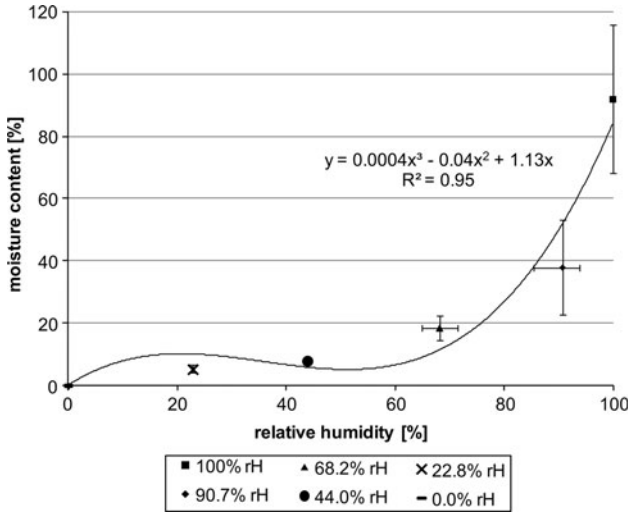

Fig. 4 Desorption of bark samples: moisture content of bark samples was plotted against the relative humidity (rH) for each step of drying. The *vertical error bars* show the standard deviation of the moisture content, *horizontal error bars* show the range of relative humidity of each storage condition. The formula of the polynomial interpolation and regression coefficient are inserted in the figure. Due to the calculation procedure used at a relative humidity of 0% a moisture content of 0% is found, in reality the moisture content of oven-dried samples ranges between 0.5 and 1.0% [19]

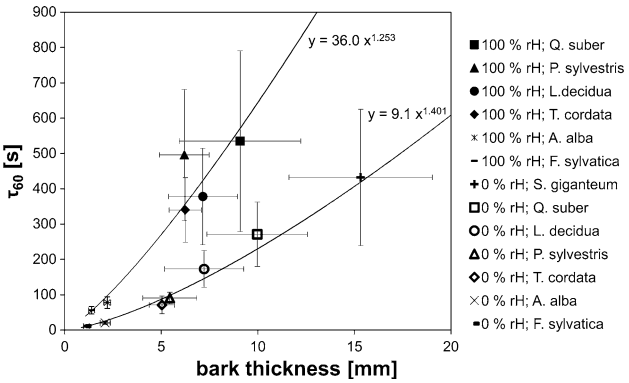

Fig. 5 τ_{60} plotted against bark thickness. Mean values of each tree species are shown. *Vertical and horizontal error bars* represent standard deviation of τ_{60} and bark thickness, respectively. For regression analysis all individually measured values were used; regression equations are given in the figure. Data for bark samples of *S. giganteum* stored at 100% rH are not given as these samples did not reach τ_{60} within the test period of 21 min

Table 1 Analysis of interspecific differences of bark thickness (D) and τ_{60} in the seven tested tree species.

		F. sylvatica	*A. alba*	*T. cordata*	*P. sylvestris*	*L. decidua*	*Q. suber*	*S. gigantuem*
F. sylvatica	D		*	***	***	***	***	***
	τ_{60}		Ø	+++	++	+++	+++	+
A. alba	D	**		***	***	***	***	***
	τ_{60}	**Ø**		+++	++	+++	+++	+
T. cordata	D	***	***		Ø	Ø	**	**
	τ_{60}	+++	+++		Ø	++	++	+
P. sylvestris	D	***	***	**Ø**		Ø	**	**
	τ_{60}	+++	+++	**Ø**		+	++	+
L. decidua	D	***	***	**Ø**	**Ø**		Ø	**
	τ_{60}	+++	+++	**Ø**	**Ø**		Ø	Ø
Q. suber	D	***	**	**Ø**	**Ø**	**Ø**		Ø
	τ_{60}	++	++	**Ø**	**Ø**	**Ø**		Ø

Values in bold samples stored at 100% rH, *values not in bold* oven-dried samples

*/+ Less significant, **/++ significant, ***/+++ highly significant, Ø no significant differences

Data for bark samples of *S. giganteum* stored at 100% rH are not given as these samples did not reach τ_{60} within the test period of 21 min

accordance with the results derived from the best subset regression (see below), our data can also be described by a linear fit ($\tau_{60} = 61.9\,D$ with $R^2 = 0.75$ for wet bark and $\tau_{60} = 26.0\,D$ with $R^2 = 0.87$ for dry bark). However, the lower goodness of fit of the linear regression indicates a better accordance of our data with a power function correlation.

The best subset regression including the independent variables bark thickness D (mm), bark structure s (–), and bark density ρ (g/cm^3) describes 94.6% of the dependent variable ($\tau_{60} = -251.5 + 73.1\,D + 118.5\,s + 246.9\,\rho$, $R^2 = 0.946$) for wet bark and 95.1% of τ_{60} ($\tau_{60} = -64.0 + 26.4\,D + 33.3\,s + 34.2\,\rho$, $R^2 = 0.951$) for dry bark. Including only D and s, 93.7% of τ_{60} can be described for wet bark ($\tau_{60} = -26.6 + 67.7\,D + 56.7\,s, R^2 = 0.937$) and 95.0% for dry bark ($\tau_{60} = -37.4 + 25.6\,D + 23.0\,s$, $R^2 = 0.95$). When only D and ρ are included, 93.1% of τ_{60} can be described for wet bark ($\tau_{60} = -67.8 + 70.0\,D + 33.5\,\rho$, $R^2 = 0.931$) and 94.9% for dry bark ($\tau_{60} = -12.3 + 25.5\,D - 29.1\,\rho$, $R^2 = 0.949$). When only D is included in the regression model, the predictability of τ_{60} only slightly decreases if at all to 93.1% ($\tau_{60} = -44.8 + 69.1\,D$, $R^2 = 0.931$) for wet bark and 94.8% ($\tau_{60} = -33.3 + 26.5\,D$, $R^2 = 0.948$) for dry bark.

Bark structure

The s-values as a measure of the degree of structuring of the bark of the tested tree species are shown in Fig. 6. Statistical analysis of interspecific differences of bark structure reveals two groups of trees. *F. sylvatica*, *A. alba*, and *T. cordata* do not differ from each other significantly in their bark structure, so they can be clustered to a group of trees with a low surface structuring of their bark. *L. decidua*, *P. sylvestris*, *Q. suber*, and *S. giganteum* also do not differ significantly in bark structure. Therefore, these species can be clustered into a second group of trees, showing a pronounced surface structuring of their bark. Differences of bark structure between these two groups are highly significant.

Bark density

Mean values of bark density (Fig. 7) range from 0.71 g/cm^3 (*F. sylvatica*) to 0.23 g/cm^3 (*S. giganteum*). Interspecific differences are highly significant for all species pairs with the exception of *F. sylvatica*/*A. alba* and *L. decidua*/*P. sylvestris*, which show no significant differences.

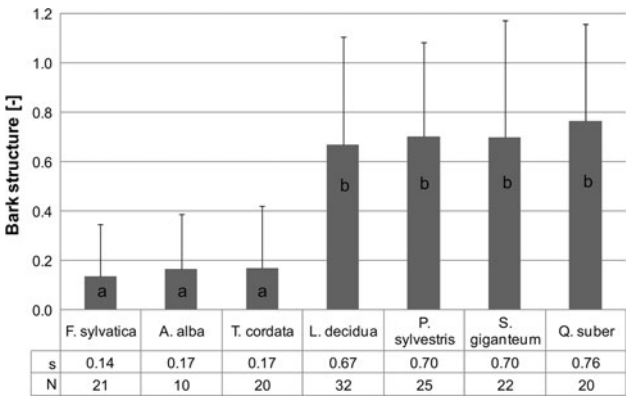

Fig. 6 Mean values and standard deviations of s as a measure of the surface structure of the bark of the tested tree species; s mean values of bark structure, N number of tested samples

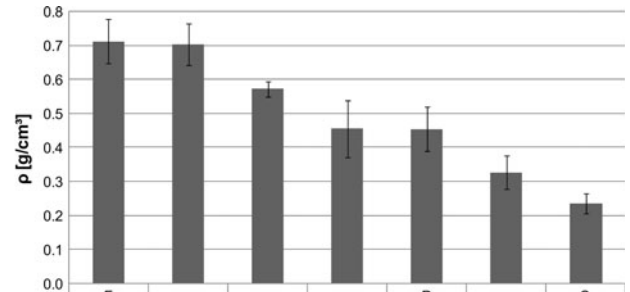

	F. sylvatica	A. alba	T. cordata	L. decidua	P. sylvestris	Q. suber	S. giganteum
ρ [g/cm³]	0.71	0.70	0.57	0.46	0.45	0.33	0.23
N	14	22	23	20	23	30	26

Fig. 7 Mean values and standard deviations of bark density ρ of the tested tree species; ρ mean values of bark structure, N number of tested samples

Modeling of dry bark

Figure 8 shows the time, τ_{60}, to reach 60 °C at the inner side, depending on the parameters A and B. The dependence on A, which is mainly influenced by the thermal conductivity, is much stronger than the influence of the parameter B, which is mainly influenced by the inner heat transfer coefficient.

Figure 9 shows the residuum of the optimization function. The residuum strongly depends on the heat conductivity. If the thermal conductivity, λ_0, is too low, τ_{60} is never reached which causes the strong increase for low λ_0. For high lambda the residuum goes towards a constant value. The residuum depends only weakly on the choice of the heat transfer coefficient α_{inner}.

The optimal values are

$$\lambda_0 = 0.17\,\text{W/mK}$$
$$\alpha_{\text{inner}} = 0.4\,\text{W/m}^2\text{K}$$

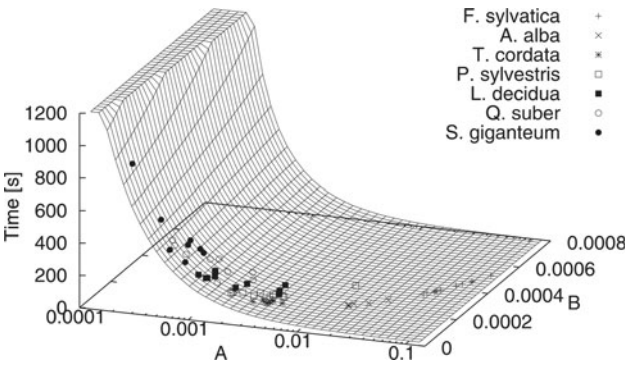

Fig. 8 τ_{60} vs. $A = \frac{\lambda}{\rho c_p D^2}$ and $B = \frac{\alpha_{\text{inner}}}{\rho c_p D}$ for dry bark. To plot the experimental results, the optimized parameters of λ_0 and α_{inner} are already used

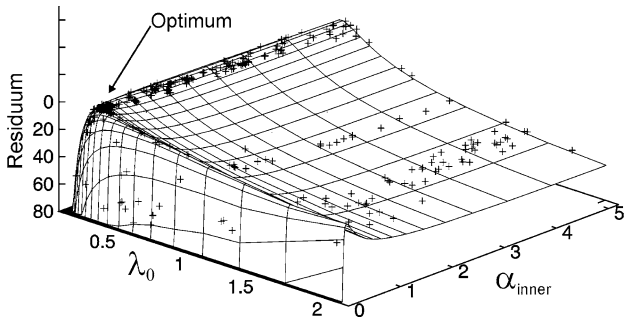

Fig. 9 Residuum versus λ_0 and α_{inner} for dry bark. The diagram is plotted upside-down to better show the optimum. The *crosses* are the trials of the genetic algorithm

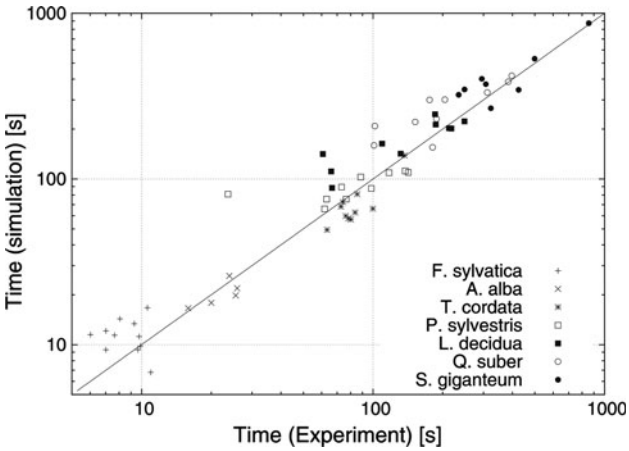

Fig. 10 Comparison of experimental times and simulated times (τ_{60}) in log–log-scale for dry bark

Figure 10 shows the comparison of the experimental and the calculated τ_{60}; due to the wide range a log–log scale is used. The basic trend is described quite well while a scatter remains, which is evenly spread around the range. This might be due to experimental uncertainties or due to not considering the inner structure of the bark in the model. In Fig. 11, the experimental and the calculated τ_{60} are compared as a function of bark thickness.

Discussion

The moisture content of bark is highly influenced by the weather. Precipitation data for the time preceding sampling indicates that the bark moisture content of the fresh samples was typical for that time of year (early August). The values of moisture content of fresh bark found in our studies correspond to those measured by Vines [14]. The polynomial curve determined as model of the course of desorption of bark (Fig. 4) is similar to that of wood found

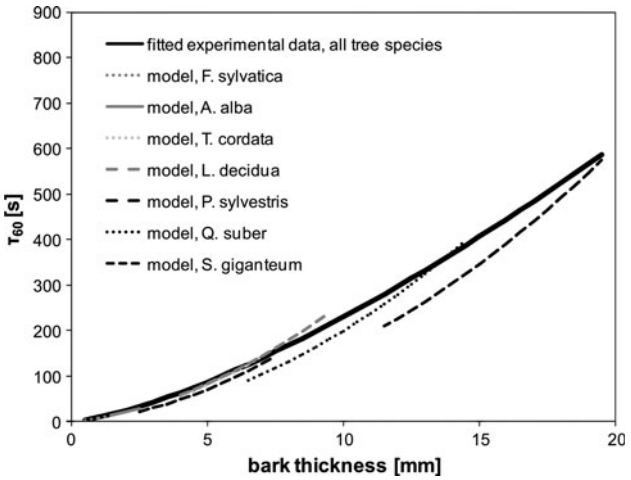

Fig. 11 Comparison of the experimental data for dry bark fitted for all seven tree species (see Fig. 5) with the simulation data of each tree species

by Knigge and Schulz [19] and allows adjusting the moisture content of the bark between 0 and 92% by choosing the respective relative humidity for storage. The latter corresponds to the value of fresh bark in good approximation.

The chosen maximum period of time for the experimental surface fire simulation (21 min) exceeds considerable the typical duration of surface fires which is about 2–9 min [8, 14]. This ensures that our test protocol allows simulating the influence of extraordinary long-lasting surface fires and therefore to test the fire resistance of bark of the different tree species even for exceptionally long surface fires. The present study simulated surface fires also with regard to flame lengths very well, since bark samples were exposed to the Bunsen burner flame at a height typical of flame lengths found in surface fires [20]. Furthermore, the mean value of flame temperatures of the Bunsen burner during surface fire simulations was close to those of typical surface fires [3].

The high predictability of τ_{60} for samples of all tree species by including only bark thickness in the best subset regression describing the experimental results supports the conclusion that a tree's fire resistance is mainly determined by its bark thickness independent of the tree species examined for a given bark moisture content (Fig. 5). Thus, a tree's fire resistance depends on its ability to build up a bark within one fire period which is thick enough to survive a surface fire. Our data suggest that a better resistance against surface fires has evolved in tree species which are more often exposed to wild fires in their natural habitat resulting in higher τ_{60}-values compared to species growing in habitats with low probability of wild fires. Other physical and structural parameters that may influence the fire resistance of bark are bark density and the surface structure of bark. When also including bark structure into the regression model, the predictability of τ_{60} only slightly increases. The same accounts for including all three independent variables, namely bark thickness, bark structure, and bark density. The consideration of quite high R^2 also for a linear model when describing the influence of bark thickness on τ_{60} allowed the use of a simplified regression model analyzing only linear correlations.

Qualitative descriptions of bark structure are abundant in the literature [21], but only few quantitative measures are used. Therefore, in this study s was introduced as a quantitative measure of the bark structure. Uhl and Kauffman [12] found that the external bark structure appears to influence external bark temperatures and might therefore also affect heat flow to the cambium. While Fahnestock and Hare [22] question whether fissures in the bark are weak points with regard to fire resistance as less intense heating in fissures may offset the effect of thinner bark, Nicolai [23] even attributes a positive influence on heat insulation to highly structured bark. Our results show that bark density decreases with increasing τ_{60}-values, suggesting that a less dense bark type with internal "air spaces" may be advantageous for an increasing fire resistance by additional insulation effects due to the internal air spaces. The same holds for the surface structure of bark which becomes more pronounced (mirrored by higher s-values) with increasing fire resistance. Additional analyses of these two parameters by further examination of bark cross sections with light and electronic microscopy will help to a better understanding as to their significance for fire resistance in bark.

Thermal insulation of tree bark and its interspecific variation with bark thickness can be described in good approximation with a simple one-dimensional volume model including measured values for outer and inner temperature, bark density, and bark porosity and assumptions for heat capacity, heat transfer coefficient, and thermal conductivity of air from literature. The tree species dependent variation of thermal conductivity of bark with porosity was modeled with the Eucken model. The model allows for a better understanding of the internal heat transfer processes and insulation capacity of (dry) bark. It proves that the experimental findings of a dependency of heat insulation from bark thickness over all tested tree species is in accordance with basic physical models for heat transfer.

Conclusion

The main parameter determining a tree's fire resistance for a given bark moisture content is the bark thickness. Bark density and bark structure only contribute to a smaller

degree to the fire resistance of bark. These results gathered from forest fire simulations in the lab can be described by a simple one-dimensional mathematical model in good approximation.

The bark itself is used by man for centuries already. It is used as construction material for heat and sound insulation. Its application as a heat insulation material reaches from flame-retardant particleboards [24] to heat insulation of intercontinental ballistic missiles [25]. For these purposes primarily the bark of the Cork Oak was used untreated or mixed with additives for ensuring an even better fire protection. Often this natural material is favored over technical insulation materials due to its good heat insulation and sound damping properties and its ability to retain humidity and thus to contribute to an improved indoor climate.

Apart from the usage of bark itself, these favorable properties could be maintained and combined with the established operating principles of current technical heat insulation materials by using bark as a concept generator for innovative bio-inspired technical thermal insulation and fire-stopping materials. Already in 1965, the potential of bark as a biological role model for an insulating board due to its numerous air cells and the abundance of cork was mentioned by Hare [26]. A biomimetic approach could be based on the external and internal meso- and microstructure, physical properties, and chemical composition of bark from highly fire resistant tree species [27]. In our opinion, the most promising approaches are to transfer findings as to the surface structure, the internal meso- and microstructure and the chemical composition of tree barks with good fire resistance to innovative biomimetic materials. A suitable surface structuring combined with internal structuring providing air spaces may contribute to an improvement of the heat insulation and fire stopping behavior of technical materials and additionally considerably reduce their weight. Additionally, technical thermal insulation materials featuring a self-adaptive moisture content by a release of water at higher temperatures might enhance its heat insulating quality in case of need and also improve its fire-stopping behavior by making use of the high amount of energy needed for the phase transformation of water from liquid to gas state. Due to the bactericidal and fungicidal properties of the phenolic components abundant in natural bark a biomimetic material including such chemical components would not be prone to mold even at higher moisture content. Water necessary for an improved fire-stopping behavior could also be encapsulated in micro-spheres, releasing the water only in the case of emergency, i.e., above a critical temperature threshold. The phenolic components in natural bark also contribute themselves because of the inflammability to the fire-stopping behavior found in many tree barks. In order to make full use of the inspiration and transfer potential provided by tree bark for biomimetic heat insulation and fire-stopping materials additional investigations on different hierarchical levels as to the functional morphology and biochemistry of tree barks are needed.

Acknowledgements We thank Julia Mergner for her assistance in examining bark density, and Rudolf Hog from the Garten- und Tiefbauamt Freiburg, as well as Wolfgang Lay, Dieter Rahm and Hans Bauer for providing plant material. We also thank Andreas Liehr for his support with the statistical analysis of the experimental data.

Appendix

See Table 2.

Table 2 Number of tested samples, *N*, mean values and standard deviations of bark thickness, and τ_{60}

Tree species	*N*		Bark thickness (mm)		τ_{60} (s)	
	100% rH	0% rH	100% rH	0% rH	100% RH	0% rH
F. sylvatica	10	11	1.39 ± 0.16	1.11 ± 0.15	56.1 ± 10.6	11.4 ± 2.7
A. alba	5	5	2.20 ± 0.18	2.09 ± 0,26	77.9 ± 16.5	20.4 ± 3.7
T. cordata	10	10	6.25 ± 0.84	5.04 ± 0.65	340.1 ± 91.5	71.3 ± 25.3
P. sylvestris	15	10	6.20 ± 1.29	5.44 ± 1.40	496.1 ± 185.4	90.8 ± 16.5
L. decidua	12	10	7.15 ± 1.78	7.22 ± 2.04	378.3 ± 136.6[a]	173.2 ± 51.8
Q. suber	10	10	9.08 ± 3.15	9.98 ± 2.60	535.1 ± 255.8	271.6 ± 91.2
S. giganteum	11	11	32.18 ± 8.88	15.32 ± 3.71	>1260	432.4 ± 193.2[a]

[a] The values of τ_{60} for *L. decidua* and *S. giganteum* were calculated excluding the experiments where τ_{60} was not reached in 21 min, and therefore represent lower estimates

References

1. Goldammer JG (1994) In: Feuer in der Umwelt: Ursachen und ökologische Auswirkungen von Vegetationsbränden; Konsequenzen für Atmosphäre und Klima; Arbeitsbericht 1992–1994/ Arbeitsgruppe Feuerökologie und Biomasseverbrennung, Max-Planck-Institut für Chemie, Abteilung Biogeochemie, Freiburg, p 3
2. Goldammer JG (1998) In: Proceedings, first baltic conference on forest fires, Radom-Katowice, Poland, p 59
3. Richter M (1997) Allgemeine Pflanzengeographie. Teubner, Stuttgart
4. Prakash A, Gupta RP (1999) Int J Remote Sens 20:1935
5. Van Mantgem P, Schwartz M (2003) For Ecol Manag 178:341
6. Dimitri L (1968) Holz Roh Werkst 26(3):95
7. Hare RC (1965) J For 63(4):248
8. Hengst GE, Dawson JO (1994) Can J For Res 24(4):688
9. Pinard MA, Huffman J (1997) J Trop Ecol 13:727
10. Gill AM, Ashton DH (1968) Aust J Bot 16:491
11. Martin RE (1963) For Prod J 13:419
12. Uhl C, Kauffman JB (1990) Ecology 71(2):437
13. Harmon ME (1984) Ecology 65(3):769
14. Vines RG (1968) Aust J Bot 16(3):499
15. Grammel R (1989) Forstbenutzung. Verlag Paul Parey, Hamburg und Berlin
16. Simpson W, TenWolde A (1999) In: Wood handbook—wood as an engineering material. General technical report FPL; GTR-113. Department of Agriculture, Forest Service, Madison, WI, US, p 3-1
17. Press WH, Teukolsky SA, Vetterling WT, Flannery BP (1992) Numerical recipes in FORTRAN, 2nd edn. Cambridge University Press, Cambridge
18. Carroll DL (2001) A genetic algorithm in Fortran Version 1.7a. www.cuaerospace.com. Accessed Oct 2009
19. Knigge W, Schulz H (1966) Grundriss der Forstbenutzung. Verlag Paul Parey, Hamburg und Berlin
20. Wade DD (1993) Int J Wildland Fire 3(3):169
21. Junikka L (1994) IAWA J 15(1):3
22. Fahnestock GR, Hare RC (1964) J For 62:779
23. Nicolai V (1989) Oecologia 80:421
24. Megraw RA (1976) US Patent 3,996,325
25. Hovey RW (1965) J Spacecr 2(3):300
26. Hare RC (1965) J For 63:248
27. Bauer G, Speck T, Liehr AW, Speck O (2009) In: Thibaut B (ed) Proceedings of the 6th plant biomechanics conference. French Guyana, France, ECOFOG Cayenne, p 482